A Molecular-Based Authentication and Authorization for Internet of Things Systems

Zhirui Lu, Osama Amin, and Basem Shihada
Computer, Electrical and Mathematical Sciences & Engineering (CEMSE) Division,
King Abdullah University of Science and Technology (KAUST),
Thuwal, Makkah Province, Kingdom of Saudi Arabia
Email: {zhirui.lu, osama.amin, basem.shihada}@kaust.edu.sa

***Abstract*—Integrating environmental and health information in the authentication and authorization processes is challenging in the Internet of things (IoT) systems using only wireless radio communications. Recent research plans for IoT future networks shed light on the need for developing new authentication techniques suitable for health care and environmental use cases. To this end, we propose a novel molecular keys (MKs)-based authentication system that uses molecules as data carriers while considering the receiver's types, concentration, and arrival time. To facilitate our proposal, we built a MK generator and detector. The system achieved a decoding accuracy of 86% for sending bit sequences within a distance of 1m. The proposed method can also accommodate dynamic authentication and authorization changes across time and places, emerging marketing applications, and evolving human activities.**

***Index Terms*—Internet of things (IoT), Molecular communication, authentication, authorization, molecular keys.**

I. Introduction

Information and communication technology have passed through several tremendous leaps throughout the previous decades. In this regard, we have witnessed a notable evolvement of the wireless communication networks from voice-based networks passing by data-based networks and reaching now the age of object-based networks. The current Internet-of-things (IoT) networks merge physical and digital environments, which requires several characteristics such as connectivity, heterogeneity, flexibility, scalability, self-organization, limited resources, sensing, and intelligence. Thus, the associated authentication and authorization techniques should be dynamic where continuous mentoring and user interactions analysis are necessary to re-validate the connected nodes' legitimacy. It is worthy to note that extracted featured data can not only be digital data, but it can also be environmental and body-related data [1].

Authentication is the process or action of verifying the identity of a user, process, or entity. To perform authentication, the user needs to supply evidence to support its identity claim, with every piece of the evidence called a factor. The most traditional yet commonly used authentication factor is the password, which is a string that only the user knows. Based on the source, authentication factors can be classified into three categories: knowledge (something the user knows, such as password, PIN, and SMS code), ownership (something the user has, such as USB security token and RFID smart card), and inherent characteristics (user's features, such as fingerprint, iris, and typing pattern). Besides using only one factor for authentication, multiple factors can also be used together to improve security. In multi-factor authentication, any missing or incorrect factor will cause the authentication process to fail; thus, the identity is only verified when all factors are correctly applied [2].

Although multiple authentication factors have been created to accommodate different use cases, they struggle to incorporate environmental and human health information. For example, in industrial biochemistry, current authentication methods are used to limit entering specific labs or areas to avoid contamination. However, individuals may be subjected to undesirable substances due to leakage or contamination, for example. Thus, we need a compatible authentication factor to detect such cases, which cannot be achieved using electromagnetic (EM) based communication systems such as RFID, smart cards, and others. Recently, the Internet working group highlighted the need to establish new authentication methods in IoT networks while preparing for the 6G standarization. Specifically, they highlighted some use cases such as health care monitoring including breathing/heart rate detection [3]. Such cases require developing unconventional compatible authentication techniques that are suitable for physical world interaction. While EM-based communication systems are having difficulties interacting with the physical world, molecular communication (MC) uses molecules to carry information [4]; thus, it can work efficiently with several physical and biological environments [5].

Authentication via molecular keys (MKs) allows utilizing environmental/health information to design a biocompatible security system and launch enhanced services. Indeed, motivated by the dynamic changes of authorization across time and places, emerging marketing applications, and evolving human activities, it is beneficial to consider another level of authentication across a molecular network. MKs can be naturally chosen from a specific environmental molecular structure or a volatile organic compound (VOC) associated with a human health and activity [6], [7]. Moreover, the MKs can be artificially generated to support several everyday applications. Throughout the rest of this paper, we design and build an MK generator and detection system to be implemented as a side authentication factor. We build the prototype

using a programmable VOC sprayer to generate molecular sequences that can be detected using a photoionization detector (PID) that are suitable for industrial environment. Then, we extensively evaluate multiple Machine Learning (ML) and Deep Learning (DL) classification models with different data normalization and feature engineering combinations to decode the transmitted MKs.

II. Molecular Authentication: Opportunities and Challenges

This section discusses possible applications motivated by the unique features and advantages of the proposed MK-based authentication. Then, we highlight some challenges that should be addressed in future system implementations.

A. Potential Use Cases

Biochemical Applications. Although it is possible to implement the existing authentication methods to grant or deny access based on visited industrial locations, it is not possible to use the contact of a specific substance to trigger these radio-frequency-based systems. However, by integrating appropriate MC detectors, such as PID, into handheld devices, the system can monitor the nearby biochemical compounds and use the predefined MKs (type and concentration) to check the authentication and grant permission.

In several industrial locations, it is either unsafe to use radio-frequency-based systems to avoid hazards (e.g., fire) or inadequate to use them in some environments such as tubes. Therefore, generating artificial compatible MKs with appropriate fluid flows can safely authenticate industrial processes and deal with different chemical substances.

Human-centric Applications. Human health and dietary habits can be easily monitored by the exhaled VOC [6]; thus, we can use the proposed MKs-based systems for authentication and monitoring daily human activities. For example, the system can limit some human activities if the alcohol level in the breath exceeds a specific threshold. Moreover, the exhaled VOC profile can be studied, trained, and used to identify viral infection particles and possibly use such information to develop pandemic mitigation authentication policies. Also, the system can allow practicing sports or using gym equipment if the health condition is suitable based on the exhaled VOC measurements.

Marketing Industrial Applications. It is possible to use MKs for marketing purposes to register rewards, which can be used to get benefits such as accessing high-speed networks and special VIP zones. Specifically, since all marketing malls use air fresheners, we propose using artificial MKs impeded in them. Then, the customers can collect the keys by visiting the stores or specific supermarket lanes, which requires spending more time thanks to the slow propagation features of MC channels. Thus, the merchants can have more chances to show their goods and attract customers.

B. Implementation Challenges

To implement the MKs-based systems in our everyday life applications, we should build a robust system that can operate under different conditions and mitigate several challenges. In the following, we summarize the main issues that can impede the implementation of the proposed system.

Dynamic Environments. The system can be affected by ambient environmental circumstances such as ventilation, interfered VOCs, and pedestrian flows, which should be considered in system modeling. Also, appropriate system implementation and detection algorithms need to be investigated to mitigate these side effects.

Regulatory Compliance. The systems that use artificial MKs should consider carefully any conditions regarding the environment. The adopted VOCs in the industrial environment should meet safety constraints and do not affect the production quality. Regarding the usage in public areas, the circulated air should be suitable for humans without causing any health problems.

Scalability. Implementing the system on a large-scale requires considering the design of long MKs, which needs using appropriate system components, protocol design, and detection algorithms. Also, accommodating multiple receiver and enabling the broadcasting feature are important feature that requires careful consideration such as different range and directions.

III. System Overview

This section gives an overview of the proposed prototype and associated system architecture used to generate and detect the MKs. As shown in Fig. 1, we show the system components, including the transmitter, receiver, modulation, as well as system testing to identify range limits.

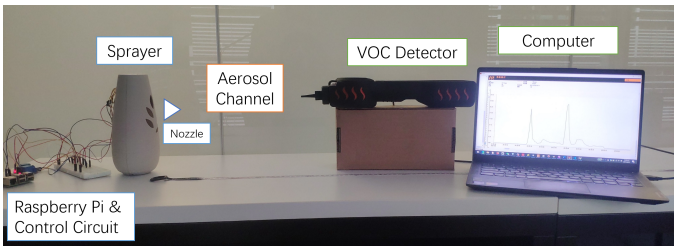

Fig. 1: The MKs generation and detection prototype.

A. Transmitter and Receiver

We build the transmitter as a programmed VOC sprayer consisting of a mechanical sprayer connected to a small motor through gears. An MK is transmitted by the sprayer using a custom script on a connected Raspberry Pi that controls a motor via relays. Commodity air freshener cans can be used as VOC source, where Ethanol is the main component of the ingredients list. The motor rotates and presses the can for a certain amount of time to release some VOC molecules, then rotates reversely to stop releasing. The Raspberry Pi connectivity and flexibility is the key to manipulate the MKs generator via a remote connection. We use a photoionization VOC detector at the receiver side to measure the VOC concentration. This detector can detect a large spectrum of VOCs

in a relatively short time (as fast as 1 sample per second) with a wide range of detection from 0.1 ppm to 5000 ppm. As a continuous stream of readings, the VOC concentration data can then be stored and retrieved from the detector for processing.

We built the whole system in a room with minimal human activity during the experiment, without any natural or artificial airflows. The distance and the alignment between the sprayer's sprinkler and the detector's nozzle can be adjusted.

B. Molecular Key Modulation

The MKs consist of a repeated sequence of ones and zeros modulated using the on-off keying scheme, where the sprayer is turned on only during the transmission of bit "1" duration. In the following, we design the system to generate 8 keys using 3 bits; however, an extended version while using more bits is also possible. To overcome the high system memory and slow propagation, as well as reducing the need for external synchronization between the transmitter and receiver, a simple communication protocol is used, as shown in Fig. 2. A pilot bit of "1" is prepended to the bit sequence to indicate the start of transmission. The bit duration t_{bit} is assumed to be known at both ends. The transmitted symbol conatins the pilot bit and three key bits, which are periodically repeated after waiting idle period t_{idle} to minimize the inter-symbol interference.

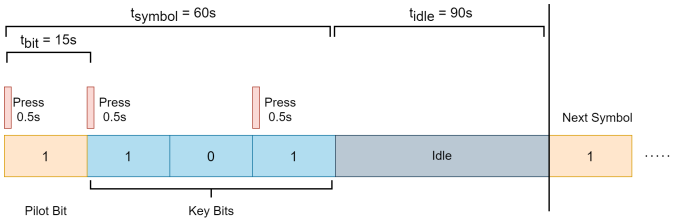

Fig. 2: Modulation of the key 101

At the receiver side, the receiver operates under three states: idle, waiting, and receiving, as illustrated in Fig. 3. The receiving procedure starts at the idle state, monitoring the VOC concentration and looking for a drastic change to detect the pilot bit, which comes after some silence time that is greater than or equal to t_{idle} by comparing the difference of current reading and the average reading of last 5 seconds to a predefined threshold. Then, it transits into a waiting state for a bit interval (t_{bit}) till the end of the pilot bit duration. After that, the receiver transits into a receiving state, in which it records the received VOC concentration for a symbol interval (t_{symbol}) to detect the transmitted key. After the transmission finishes, the receiver goes back to the idle state, and the VOC concentration segments are sent into a classification model to recover the transmitted bits.

C. System Testing

To assess the MK generation and detection system under the limited aerosol transmission channel, we conduct several experiments to define the system operating conditions and identify the limitations. The limitations mainly come from 2

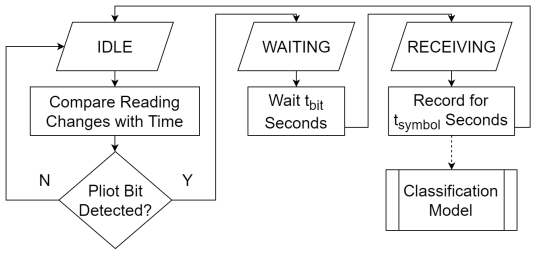

Fig. 3: Receiver state transition.

aspects, signal strength and interference, as can be observed from the following experiments.

Observed VOC Concentration. We start by studying the VOC concentration observed at the receiver side after sending the key "101" as shown in Fig. 4. Despite the short VOC release press time, the received pulse width is wider than the press time due to the dispersion nature of the aerosol channel. The transmitted bits appear some spikes that can be identified and recognized as depicted in Fig. 4. Other fluctuations are due to environmental noises and channel turbulence. The previously mentioned reasons motivate us to reserve enough time between bit pressing time slots and also between the symbols, i.e., t_{idle}, to reduce the interference between adjacent bits and symbols.

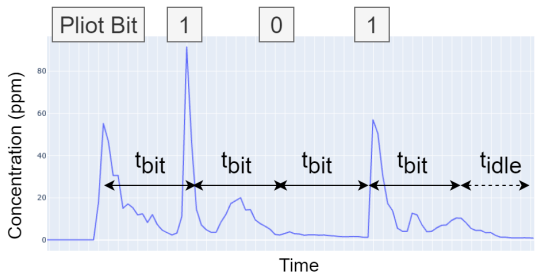

Fig. 4: Received VOC concentration of key 101.

Impact of Distance. We send the key "111" with the sprayer and the detector aligned and measure the received signal strength in terms of the average VOC concentration versus different transmission range as shown in Fig. 5. We observe relatively high concentration measurements for small distances, allowing the keys to be detected efficiently. As the receiver moves further away, the measured VOC concentration decreases significantly due to the diffusion nature of the aerosol channel and the corresponding signal loss with the distance. According to the depicted results in Fig. 5 and the noise levels in Fig. 4, the adopted setup can operate satisfactorily for distances up to 1.5 m. However, at longer distances, the slow diffusion of the aerosol channel results in low values of received concentration compared to the environmental noise; thus, individual spikes may not be observed while the decoding is hardly possible.

Impact of Alignment. To understand the impact of alignment, we consider different angles between the spraying direction and the receiver at a distance of 0.7 m, using the

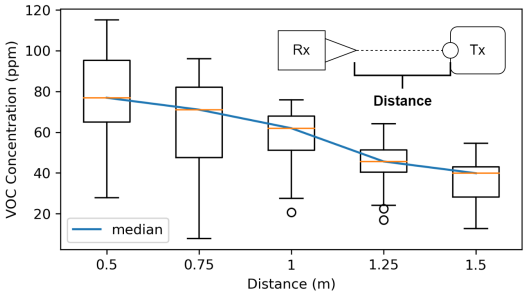

Fig. 5: Effect of distance on VOC concentration.

same key “111". The value of angle quantifies the deviation of alignment. Since the released VOC mostly exists along the nozzle axis, the amount of VOC arrived at the detector decreases as the angle increases. Based on the results in Fig. 6 and the noise level shown in Fig. 4, the system can maintain a relatively good signal level within 20° angles range.

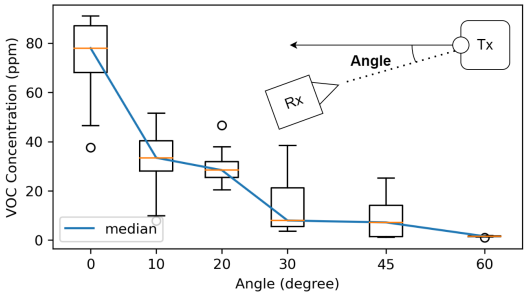

Fig. 6: Effect of alignment on VOC concentration.

IV. Problem Description

After generating different MKs and recording the VOC concentration at different time instants, the main problem becomes recovering these keys from the detected VOC concentration readings, similar to the depicted one in Fig. 4. The recovery process is done via two steps: First, segmenting the readings then, decoding the data.

Segmentation. After getting the VOC concentration readings for a time span of T timesteps, $y_1, y_2, \ldots, y_T$, we isolate the reading segment, $\mathbf{Y}$, related to the key. The elements of $\mathbf{Y}$ are $Y_k[j]$, which represents the readings on j-th timestep of the k-th bit in the sequence.

Decoding. To decode $\mathbf{Y}$ data into the estimated key bits, we consider it a classification problem under variable channel and noise conditions. We perform the classification using learning algorithms that need extensive experimental training phases. Multiple classification models in ML can be applied to this problem, but some of them require larger dataset for better generalization. To address this problem efficiently, we first model the received bit concentration function based on several experimental measurements in the following section. Then, we use the model to generate a simulated dataset and train different classification learning models in Section 5.

V. VOC Concentration Modeling

In this section, we model the received VOC concentration by fitting theoretical models to our experimental data. We use the model proposed in [8] that has shown to be suitable for molecular channel characteristics.

Modeling Single Release. The received VOC concentration of a single transmitted pulse is modeled as a function in the time t as [8],

$$\lambda(t) = \begin{cases} \kappa\sqrt{\frac{c}{2\pi t^3}}\exp\left[-\frac{c(t-\mu)^2}{2\mu^2 t}\right] & t > 0 \\ 0 & t \leq 0 \end{cases} \quad (1)$$

where κ is a proportionality constant, c and μ are channel parameter, which can be found by fitting the curve to experimental data.

Fitting Single Release. To find κ, c and μ, we conducted 30 single-release experiments for aligned sprayer and detector while allow an idle time of 120 seconds between consecutive presses to avoid signal interference. Then, we use a simulated annealing algorithm (implemented in [9]) to fit the parameters, by minimizing root-mean-square error (RMSE) between values predicted by the model and the experiment, over the time length 45 seconds at a sampling rate of 1 sample/sec. The parameters are found to be: $\kappa = 408$, $c = 71.2$ and $\mu = 11.9$. Fig. 7 shows the 30 received signal of single press versus time overlayed on the fitted model, which verifies the good approximation.

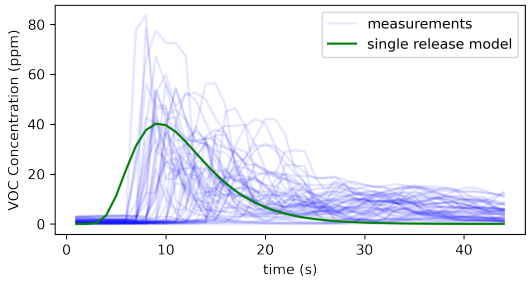

Fig. 7: Comparison between several measurements of the received single release pulse and the adopted model.

Modeling Sequence Release. Following the fitted model for the single release, we model the stream of molecular bits and develop an appropriate model. The summation of delayed versions of $\lambda(t)$ follows a Poisson distribution [8]; thus, the distribution of the received VOC concentration is written as,

$$Y_k[j] \sim \mathscr{P}\left(\sum_{i=0}^{k} x_{k-i}\lambda_i[j] + \eta\right) \quad (2)$$

where η represents an independent additive Poisson noise coming from background or the receiver, $\mathscr{P}(\xi) = \frac{\xi^y e^{-\xi}}{y!}$ is the Poisson distribution function with a parameter ξ and y is the measured value. By interpreting the parameter ξ as the amount of VOC molecules in the air near the detector, sampling from the Poisson distribution simulates the measuring of VOC concentration since Poisson distribution describes the

probability of random events happening in a given time, and molecule being captured by the detector is such an event. $\lambda_i[j]$ is the response at the j-th timestep of the current bit due to the i-th bit in the transmission and is expressed as

$$\lambda_i[j] = \lambda(\frac{i \cdot \omega \cdot \mathrm{t_{bit}} + j}{\omega}) \tag{3}$$

with ω denoting the sampling rate.

VI. Retrieving Molecular Keys

In this section, we detail the implementation of the keys decoding process from the received VOC concentrations using the previously discussed channel characterization simulation model. Covering all possible fluctuations by experiments would be impossible; thus, the simulated dataset helps the decoding models access plenty of generalized results. By viewing the decoding problem as a time series classification problem, various model configurations can be built using different models, normalization, and feature engineering techniques.

Building Simulation Dataset. We developed a customized script to simulate the transmission of different keys sequences considering randomization of time alignment, concentration amplitude, and environmental noises to simulate the VOC diffusion more realistically. To this end, we created a simulated dataset of size 10000 and adopted the segmentation procedure to capture the key sequence information.

Normalization and Feature Engineering. Before processing the received data, it is necessary to normalize them to improve the predictability and robustness. We use two normalization methods: the Z-normalization, which normalizes the data to have zero-mean and unity standard deviation values, and the min-max normalization, which normalizes the data between 0 and 1. Regarding feature engineering, we use two techniques: slope, which calculates the difference between each time step, and summary, which computes different statistics, as the maximum, minimum, variance, median, and mean.

Methods. As a univariate time series classification problem, several ML classification methods are applicable. All these methods can be categorized considering two perspectives, as shown in Table I. Firstly, the methods can be classified as to whether DL can be involved or just classic ML. Secondly, they can be classified according to whether the time semantic is preserved or not, i.e., whether the input is seen as a pure vector or a time series.

TABLE I: Methods Summary

	Preserve Time Semantic	Discard Time Semantic
Classic ML	TS-KNN[1] TS-Forest[2] RISE[3]	KNN [10]* SVM [11]* Naive Bayes* Decision Tree* Random Forest*
Deep Learning	CNN (FCN/ResNet [4])* RNN (LSTM [12]/GRU [13])* BiRNN [14] (LSTM/GRU)*	MLP [15] *

Here are some additional explanations to Table I:

- CNN is classified as "Keep Time Semantic" as it performs convolution along the time axis, thus retaining the sequence nature of a time series.
- For Bidirectional RNNs, a variant using 3 Bidirectional layers (denoted by “3Bi") is also tried.
- For MLP and CNN Methods, the implementation is based on a review paper by H. Fawaz etal [20]. CNN methods are chosen as the top 3 ranked methods according to their pairwise ranking on univariate time series classification.

For the methods with an asterisk, besides directly taking the time series as input, a variant which takes both the input sequence and its summary (as described in Feature Engineering) is also tried. For Classic ML methods, the summary is simply concatenated along with the input sequence. For DL methods, the summary is inputted as another branch, which first passes 2 fully connected layers, then a dropout layer, finally concatenated with the output from the sequence branch, before the final fully connected layer and the output layer, as shown in Fig. 8.

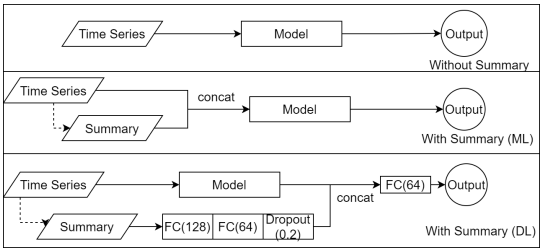

Fig. 8: Classification models with and without summary.

Training. To make a fair comparison, most models are trained in the same fashion:

- Classic ML methods: First run a grid search with 5-fold cross validation on the simulated dataset to find the best parameters, then the model is trained using the whole simulated dataset and tested on the real dataset.
- DL methods: All models use an Adam optimizer with a learning rate of 1e-3. Models can be trained at most 200 epochs on the simulated dataset, but an early stop callback is registered on the validation loss (validation set taken from simulated dataset), so the training will stop if the loss does not decrease in 10 epochs.

Some specific measures are used when the general training methods do not work well, as stated below.

- For Time Series ML methods, running grid search with 5-fold CV takes a long time, so only 10% of the simulated dataset for this stage. Later the model is still trained using the whole simulated dataset to find the best parameters.
- For FCN in CNN, AdaDelta optimizer is used instead of Adam [20].

[1]Time series KNN with dynamic time warping (DTW) [16].
[2]Time Series Forest, [17] [16].
[3]Random Interval Spectral Ensemble, [18] [16].
[4]Fully convolutional neural network & relatively deep residual network [19].

TABLE II: Top 5 Methods

Rank	ML/DL	Method	Normalization	Feature Engineering		Simulated Dataset		Sequence Release Dataset	
				Slope	Summary	Accuracy	Weighted F1	Accuracy	Weighted F1
1	DL	BiLSTM	none	✓		0.974	0.975	0.864	0.868
2	DL	3BiGRU	znorm	✓	✓	0.978	0.978	0.818	0.818
3	ML	NaiveBayes	none	✓		0.658	0.661	0.818	0.816
4	ML	kNN	none			0.980	0.980	0.818	0.814
5	DL	GRU	minmax	✓	✓	0.973	0.973	0.795	0.790

VII. System Performance Evaluation

In this section, we evaluate the decoding performance of different classification learning methods using experimentally measured data to find the best methods. We use two metrics known as accuracy and class-weighted F1, which are suitable for our multi-class classification problem. The accuracy is defined as the percentage of correct predictions on all predictions. While the class-weighted F1 is the sum of F1 scores in each class weighted by the class size that is expressed as,

$$\text{Class Weighted F1} = \sum_{i=0}^{C} \frac{N_i}{N} \text{F1}_i, \tag{4}$$

where C denotes the number of classes, N denotes the records number, N_i denotes the records number in the class i, and $F1_i$ denotes the F1 value of the class i, which is found from

$$\text{F1} = 2 \times \frac{\text{Precision} \times \text{Recall}}{\text{Precision} + \text{Recall}} \tag{5}$$

where the precision and recall are computed using true positive (TP), false positive (FP) and false negative (FN) as,

$$\text{Precision} = \frac{\text{TP}}{\text{TP} + \text{FP}} \qquad \text{Recall} = \frac{\text{TP}}{\text{TP} + \text{FN}}. \tag{6}$$

We use the sprayer to transmit all possible 3-bit digital sequences, *i.e.*, from 000 to 111, following the modulation and protocol defined previously. After receiving the data at the detector side, the corresponding segments are isolated for each bit sequence, and then different ML classification methods are tested on 44 segments. To quantify the performance of different ML classification methods, we computed the accuracy and weighted F1 metric for all methods using different normalization and feature engineering. Table II lists the best 5 methods while showing the adopted normalization and feature engineering. Among all methods, the Single Layer Bidirectional LSTM achieves the highest accuracy of 0.864.

VIII. Conclusion

This work considered an authentication factor utilizing MC, named MK to be adopted for authentication and authorization in IoT systems. Compared to traditional authentication factors, using molecules as carrier enables authentication process to interact with physical world easier, creating new possibilities and providing more flexibility to designing industrial security systems. A prototype was built to show the feasibility of purposed system, using a sprayer the transmitter and a VOC detector as the receiver. Different ML and DL techniques were considered for recovering the bits transmitted from the VOC concentration reading stream. Advantages and current limitations are discussed, with potential applications in multiple domains.

References

[1] F. H. Al-Naji and R. Zagrouba, "A survey on continuous authentication methods in internet of things environment," *Computer Commun.*, vol. 163, pp. 109–133, 2020.

[2] M. H. Barkadehi, M. Nilashi, O. Ibrahim, A. Zakeri Fardi, and S. Samad, "Authentication systems: A literature review and classification," *Telematics and Informatics*, vol. 35, no. 5, Aug. 2018.

[3] D. v. Hugo and B. Sarikaya, "The Need for New Authentication Methods for Internet of Things," Internet Engineering Task Force, Internet-Draft draft-hsothers-iotsens-ps-01, Jan. 2022.

[4] T. Nakano, T. Suda, M. Moore, R. Egashira, A. Enomoto, and K. Arima, "Molecular communication for nanomachines using intercellular calcium signaling," in *5th IEEE Conf. Nanotechnol.*, Jul. 2005, pp. 478–481 vol. 2, iSSN: 1944-9399.

[5] D. T. McGuiness, S. Giannoukos, S. Taylor, and A. Marshall, "Analysis of Multi-Chemical Transmission in the Macro-Scale," *IEEE Trans. Mol. Biol. Multiscale Commun.*, vol. 6, no. 2, pp. 93–106, Nov. 2020.

[6] M. Khalid, O. Amin, S. Ahmed, B. Shihada, and M.-S. Alouini, "Communication through breath: Aerosol transmission," *IEEE Commun. Mag.*, vol. 57, no. 2, pp. 33–39, 2019.

[7] O. Amin, H. Dahrouj, N. Almayouf, T. Y. Al-Naffouri, B. Shihada, and M.-S. Alouini, "Viral aerosol concentration characterization and detection in bounded environments," *IEEE Trans. Mol. Biol. Multiscale Commun.*, vol. 7, no. 3, pp. 185–199, Sept. 2021.

[8] N. Farsad and A. Goldsmith, "Neural Network Detection of Data Sequences in Communication Systems," *IEEE Trans. Signal Process.*, vol. 66, no. 21, pp. 5663–5678, Nov. 2018.

[9] "microsoft/nni," Jun. 2021.

[10] N. S. Altman, "An Introduction to Kernel and Nearest-Neighbor Nonparametric Regression," *The American Statistician*, vol. 46, no. 3, pp. 175–185, 1992, publisher: [American Statistical Association, Taylor & Francis, Ltd.].

[11] C. Cortes and V. Vapnik, "Support-vector networks," *Machine Learning*, vol. 20, no. 3, pp. 273–297, Sep. 1995.

[12] S. Hochreiter and J. Schmidhuber, "Long Short-Term Memory," *Neural Computation*, vol. 9, no. 8, pp. 1735–1780, Nov. 1997.

[13] K. Cho, B. van Merrienboer, C. Gulcehre, D. Bahdanau, F. Bougares, H. Schwenk, and Y. Bengio, "Learning Phrase Representations using RNN Encoder-Decoder for Statistical Machine Translation," *arXiv:1406.1078 [cs, stat]*, Sep. 2014, arXiv: 1406.1078.

[14] M. Schuster and K. Paliwal, "Bidirectional recurrent neural networks," *IEEE Trans. Signal Process.*, vol. 45, no. 11, pp. 2673–2681, Nov. 1997.

[15] Y. Freund and R. E. Schapire, "Large Margin Classification Using the Perceptron Algorithm," *Machine Learning*, vol. 37, no. 3, pp. 277–296, Dec. 1999.

[16] "alan-turing-institute/sktime," Jun. 2021, original-date: 2018-11-06T15:08:24Z.

[17] H. Deng, G. Runger, E. Tuv, and M. Vladimir, "A Time Series Forest for Classification and Feature Extraction," *arXiv:1302.2277 [cs]*, Feb. 2013, arXiv: 1302.2277.

[18] J. Lines, S. Taylor, and A. Bagnall, "Time Series Classification with HIVE-COTE: The Hierarchical Vote Collective of Transformation-Based Ensembles," *ACM Trans. Knowl. Discov. Data*, vol. 12, no. 5, pp. 52:1–52:35, Jul. 2018.

[19] Z. Wang, W. Yan, and T. Oates, "Time series classification from scratch with deep neural networks: A strong baseline," in *Int. Joint Conf. Neural Networks (IJCNN)*. IEEE, 2017, pp. 1578–1585.

[20] H. I. Fawaz, G. Forestier, J. Weber, L. Idoumghar, and P.-A. Muller, "Deep learning for time series classification: a review," *Data Mining and Knowledge Discovery*, vol. 33, no. 4, pp. 917–963, Jul. 2019, arXiv: 1809.04356.